Innovative: International Multi-disciplinary Journal of Applied Technology
(ISSN 2995-486X) VOLUME 4 ISSUE 11, 2026

IMPROVING SILK REELING EQUIPMENT TO OBTAIN HIGH-QUALITY RAW SILK FROM LOCAL SILKWORM COCOONS

Ulug‘bek Akhunbabayev
PhD, Senior Researcher, Head of the Laboratory, Uzbek Scientific Research Institute of Natural Fibers, Margilon, Uzbekistan

Fotimabonu Rustamova
PhD candidate, Namangan State Technical University, Uzbekistan

Akmal Umarov
DSc, Associate Professor of the Department of Technological Machinery and Equipment, Namangan State Technical University, Namangan, Uzbekistan

Abstract:

The quality of raw silk is determined jointly by the intrinsic properties of the cocoon and by the mechanical and thermal environment in which the filament is unwound. Local cocoon hybrids frequently show high intrinsic potential, yet raw silk reeled on ageing, mostly mechanically controlled equipment is often downgraded because of fineness variation, frequent filament breakage and elevated cleanness defects. This study presents the design, implementation and experimental evaluation of an integrated set of seven equipment improvements: cocoon sorting, staged three-zone cooking, closed-loop reeling-basin temperature control, ceramic eyelets with an optimized cross-twist unit, a photoelectric fineness sensor with automatic cocoon feeding, a load-cell based adaptive take-up, and humidity-controlled drying. The modifications were driven by a PLC-based PID controller with data logging. The structural and kinematic schemes of the improved reeling unit are presented, and its reel drive, consisting of an asynchronous motor with a frequency converter, a V-belt drive and a two-stage cylindrical gear reducer, is calculated so that the reeling speed can be set within 36-84 m/min. Five lots of locally produced cocoons were reeled to 20/22 den raw silk on a baseline machine and on the improved machine, with three replicates per lot. The improved configuration raised reelability from 71.2 % to 86.4 %, increased raw silk recovery from 34.9 % to 39.6 %, reduced the coefficient of variation of fineness from 14.2 % to 7.8 %, lowered the filament break rate by 58 %, and improved tenacity by 14.3 %, moving the product from an intermediate grade to the top commercial grade. Specific thermal energy consumption decreased by 29 %. The results show that targeted, low-cost equipment upgrades can unlock the quality potential of local cocoons without changing the raw material, and they provide design rules that can be transferred to small and medium reeling enterprises.

Keywords: silk reeling; raw silk; Bombyx mori; local cocoons; process control; PID; reelability; fineness uniformity; gear reducer; kinematic scheme.

Introduction

Silk is one of the oldest natural protein fibres used by humankind and, despite the dominance of synthetic polymers, it remains a high-value material in textiles, medicine and advanced functional systems [1]. The fibre produced by the domesticated mulberry silkworm, Bombyx mori, consists of two filaments of fibroin glued together by a sericin coat, and it combines high tensile strength with considerable extensibility, a combination that few natural or synthetic fibres can match . Fibroin accounts for roughly 70-80 % of the cocoon shell mass, while sericin accounts for most of the remainder and must be softened and partly removed during reeling and degumming. These structural characteristics explain why the way in which a cocoon is cooked, unwound and dried has a decisive influence on the quality of the raw silk that is finally delivered to weavers[2].

Raw silk production is a chain of several operations: cocoon drying and storage, sorting, cooking (softening of sericin), brushing and end-finding, reeling, re-reeling, and conditioning of the finished skeins. In each step the filament is exposed to temperature, moisture and tension, and any uncontrolled fluctuation can be transferred to the product as fineness variation, cohesion loss, neatness defects or reduced strength. A cocoon filament is several hundred to more than a thousand metres long and its linear density tapers from the outer to the inner layers of the shell, so the reeling equipment must continuously compensate for the progressive thinning of the filament by adding new cocoons at the correct moment. Where this compensation depends mainly on operator skill, the output is highly variable even when the cocoon raw material is excellent[3].

Producers that rely on locally grown cocoons face a particular challenge. Local hybrids are selected for adaptation to regional climate, feeding conditions and rearing practice, and they frequently show good filament length and shell ratio; however, their size distribution, shell compactness and sericin content differ from those of the imported or standard hybrids for which most commercially available reeling machines were originally designed. Consequently, parameters such as cooking temperature profile, basin temperature, eyelet geometry and take-up speed that are acceptable for standard material may be sub-optimal for local material. The mismatch is amplified in many small and medium enterprises, where equipment is old, temperature is regulated manually and tension is not measured at all[4].

The mechanical behaviour of silkworm silk is intrinsically variable, because it depends on the degree of molecular orientation, on the reeling speed and on the thermal history of the filament. Shao and Vollrath showed that the apparently modest strength of cocoon silk is not an inherent limitation but is strongly influenced by how the filament is drawn, and that carefully controlled forced silking can approach the performance of spider dragline silk. Jin and Kaplan, in turn, described how the processing of the protein solution in the silk gland, including shear, pH and ion changes, governs the formation of beta-sheet crystals and, therefore, the mechanical response of the finished fibre. These findings imply that a reeling system that keeps tension and temperature within narrow limits is not only a tool for convenience but also a means to preserve the fibre structure created by the insect[5].

Technical literature on silk is dominated by studies on silk fibroin as a biomaterial, regenerated fibroin films, scaffolds and sponges, and on the molecular architecture of the fibroin heavy chain gene. Reviews of the biomedical and technological uses of silk emphasize that the properties of the final material are inherited from the quality of the starting fibre . In contrast, engineering studies on the mechanics, control and instrumentation of the reeling process itself, particularly in the context of small-scale producers, are comparatively scarce. Practical manuals describe the principles of reeling and testing in detail but they do not offer a validated procedure for upgrading existing equipment so that local cocoons reach top commercial grades[6].

The objective of the present work is therefore to close this gap. We (i) analyze the causes of quality loss on a conventional reeling machine operating with local cocoons, (ii) design a package of seven equipment

improvements targeting thermal, mechanical and control weaknesses, together with the structural and kinematic schemes of the improved reeling unit and the kinematic calculation of its reel drive, (iii) implement them on a pilot reeling line equipped with a PLC-based PID controller and sensors, and (iv) quantify the effect of the upgrade on reelability, recovery, fineness uniformity, strength, grading and energy use through a replicated experimental design. The novelty of the study lies in treating the reeling machine as an integrated, instrumented system, rather than as a set of independent mechanical units, and in tuning this system specifically to the cocoon characteristics of locally produced hybrids[7-9].

Materials and Methods

Five lots of fresh, stifled and dried cocoons of locally bred Bombyx mori hybrids were obtained from the regional silkworm rearing season. Each lot contained approximately 20 kg of cocoons. Before the experiments the cocoons were stored in a ventilated room at 20-25 °C and 60-65 % relative humidity for seven days in order to equalize moisture content. For every lot, a random sample of 200 cocoons was used to determine the mean cocoon mass, shell mass, shell ratio and the proportion of defective cocoons (double, stained, thin-shelled and deformed). These descriptors were later used as covariates to verify that the differences between the baseline and improved machines could not be attributed to differences in the raw material.

Baseline reeling machine and diagnosis of quality losses

The baseline machine was a conventional multi-end reeling machine with a hot-water basin heated by steam coil, a manually operated valve, metal-coated eyelets, a mechanical cross-twist (chambon) device, a constant-speed take-up reel and a convective oven for drying skeins. Operators added cocoons by visual judgment of the filament thickness. A diagnostic trial of 15 reeling runs was carried out to identify the main sources of quality loss. During this trial the basin temperature was logged every 10 s, the filament tension was measured at the take-up using a temporary load cell, and each break event was classified as being caused by (a) cocoon defects, (b) thermal non-uniformity, (c) excessive tension, or (d) mechanical damage at guides. This classification followed the practical guidelines on reeling faults described in.

The diagnosis revealed that basin temperature fluctuated by up to ±4.5 °C around the setpoint, that tension peaks during cocoon replenishment exceeded the average tension by a factor of 2.1 to 2.6, that guide surfaces showed micro-grooves that abraded sericin and produced fuzz, and that the delay between a drop in filament fineness and the addition of a new cocoon was in many cases longer than 6 s. Together these four factors accounted for approximately 73 % of the observed filament breaks, which provided the basis for the design of the improvement package.

2.3 Design of the improved equipment

The improved machine integrates seven modules, denoted M1-M7 in Fig. 1 and summarized with their key parameters in Table 1. Module M1 is a cocoon sorting stage that separates cocoons into three size classes and removes defective ones, so that cocoons with similar filament length and fineness are combined in a single end. Module M2 replaces single-stage cooking by staged cooking in three zones, with water temperature increasing from 70 °C to 85 °C and then to 95 °C and a controlled perfusion of hot water through the cocoon bed. The graded temperature profile swells the sericin gradually, reduces the formation of hard-glued layers and facilitates uniform unwinding, which is consistent with the role of sericin in cocoon structure discussed in.

Module M3 introduces closed-loop control of the reeling-basin water temperature. A PT100 probe measures the temperature at the point of filament entry, and the PLC modulates the heating power through a proportional valve according to a discrete PID algorithm. Module M4 comprises ceramic eyelets with polished surfaces (surface roughness below 0.2 µm) and a redesigned cross-twist unit with a 90° crossing angle and adjustable distance, which increases cohesion between the baves without raising the contact pressure. Module M5 uses a photoelectric sensor that measures the optical density of the filament bundle, which is proportional to its linear density; when the signal falls below a lower threshold, a pneumatic feeder adds a pre-prepared cocoon end. Module M6 is an adaptive take-up in which the angular speed of the reel is adjusted continuously, through a frequency converter and a gear reducer,

according to the signal of a load cell, and module M7 is a humidity-controlled drying chamber for the skeins. The arrangement of the modules on a reeling position and the kinematic scheme of the reel drive are shown in Fig. 2 and described in Section 2.4.

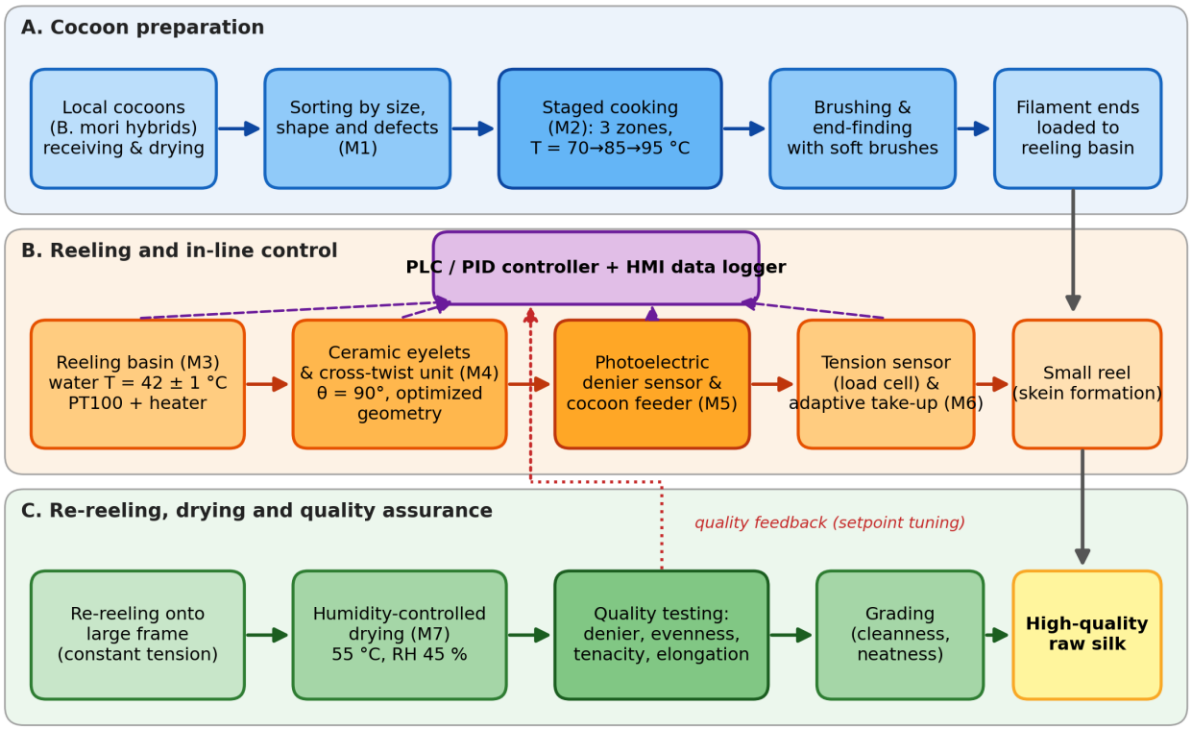


Fig. 1. Process and control architecture of the improved silk reeling line (modules M1-M7)

The control logic is based on three coupled loops: the temperature loop (M3), the fineness loop (M5) and the tension loop (M6). The PID law used in each loop is

$$u(t) = K_{\mathrm{p}} e(t) + K_{\mathrm{i}} \int_0^t e(\tau)\mathrm{d}\tau + K_{\mathrm{d}} \frac{\mathrm{d}e(t)}{\mathrm{d}t} \tag{1}$$

where $u(t)$ is the control signal, $e(t)$ is the deviation from the setpoint, τ is the integration variable and K_{p}, K_{i} and K_{d} are the proportional, integral and derivative gains. The gains were initially estimated by the Ziegler-Nichols step-response method and subsequently fine-tuned in pilot runs to minimize overshoot. The tension on the filament as it passes over a curved guide of wrap angle θ is described by the capstan relation

$$T_2 = T_1 \mathrm{e}^{\mu\theta} \tag{2}$$

in which T_1 and T_2 are the tensions before and after the guide, and μ is the coefficient of friction between filament and guide. Equation (2) shows that the exponential influence of μ makes the surface quality of eyelets a first-order design parameter: reducing μ from 0.35 (worn metal guide) to 0.18 (polished ceramic) reduces the tension increase over a total wrap angle of $\theta = \pi$ radians from a factor of 3.0 to a factor of 1.8. Finally, because the strength of silk filaments is statistically distributed [14], the breakage probability at tension σ was modelled with a two-parameter Weibull function,

$$P_{\mathrm{f}}(\sigma) = 1 - \exp\left[-\left(\frac{\sigma}{\sigma_0}\right)^m\right] \tag{3}$$

where σ_0 is the scale parameter and m is the shape parameter (Weibull modulus). A high value of m indicates narrow strength scatter. The model was used to define the tension setpoint and the maximum permitted tension peak so that the predicted breakage probability per metre of filament remained below 10^{-4}.

Table 1. Main design and operating parameters of the baseline and improved machines

Module / parameter	Baseline machine	Improved machine	Target effect
M1 Cocoon sorting	None (manual mixing)	3 size classes, defect removal	Uniform filament length
M2 Cooking	Single stage, 95 °C	3 zones, 70/85/95 °C	Gradual sericin softening
M3 Basin temperature	±4.5 °C, manual valve	42 ± 1 °C, PID	Stable unwinding
M4 Guides / cross-twist	Metal, $\mu \approx 0.35$	Ceramic, $\mu \approx 0.18$, 90°	Lower tension, less fuzz
M5 Fineness control	Visual, delay > 6 s	Optical sensor, delay < 1.5 s	Fineness CV reduction
M6 Take-up	Constant speed	Load-cell adaptive speed via FC and gear reducer	Tension peaks damped
M7 Drying	Convective, uncontrolled	55 °C, RH 45 %, controlled	Less brittleness, better hand

2.4 Equipment scheme and kinematic calculation of the reel drive

The structural scheme of one reeling position of the improved machine and the kinematic scheme of its reel drive are shown in Fig. 2. Cocoons prepared in the sorting (M1) and staged cooking (M2) stages are transferred to the reeling basin 1, where the water temperature is measured by the PT100 sensor 2 at the point of filament entry and maintained by the steam heater with proportional valve 3 (M3). The baves of seven to eight cocoons are gathered through the ceramic eyelet 5 and pass through the cross-twist (chambon) unit 6, in which the thread is crossed on itself at 90° to consolidate the baves and squeeze out water (M4). The thread then passes through the photoelectric fineness sensor 7; when its signal falls below the lower threshold, the controller 15 actuates the pneumatic feeder 4, which attaches a new cocoon end to the thread (M5). After the guide roller 8, which is mounted on a load cell (M6), the thread is laid by the traverse guide 9 onto the take-up reel 10.

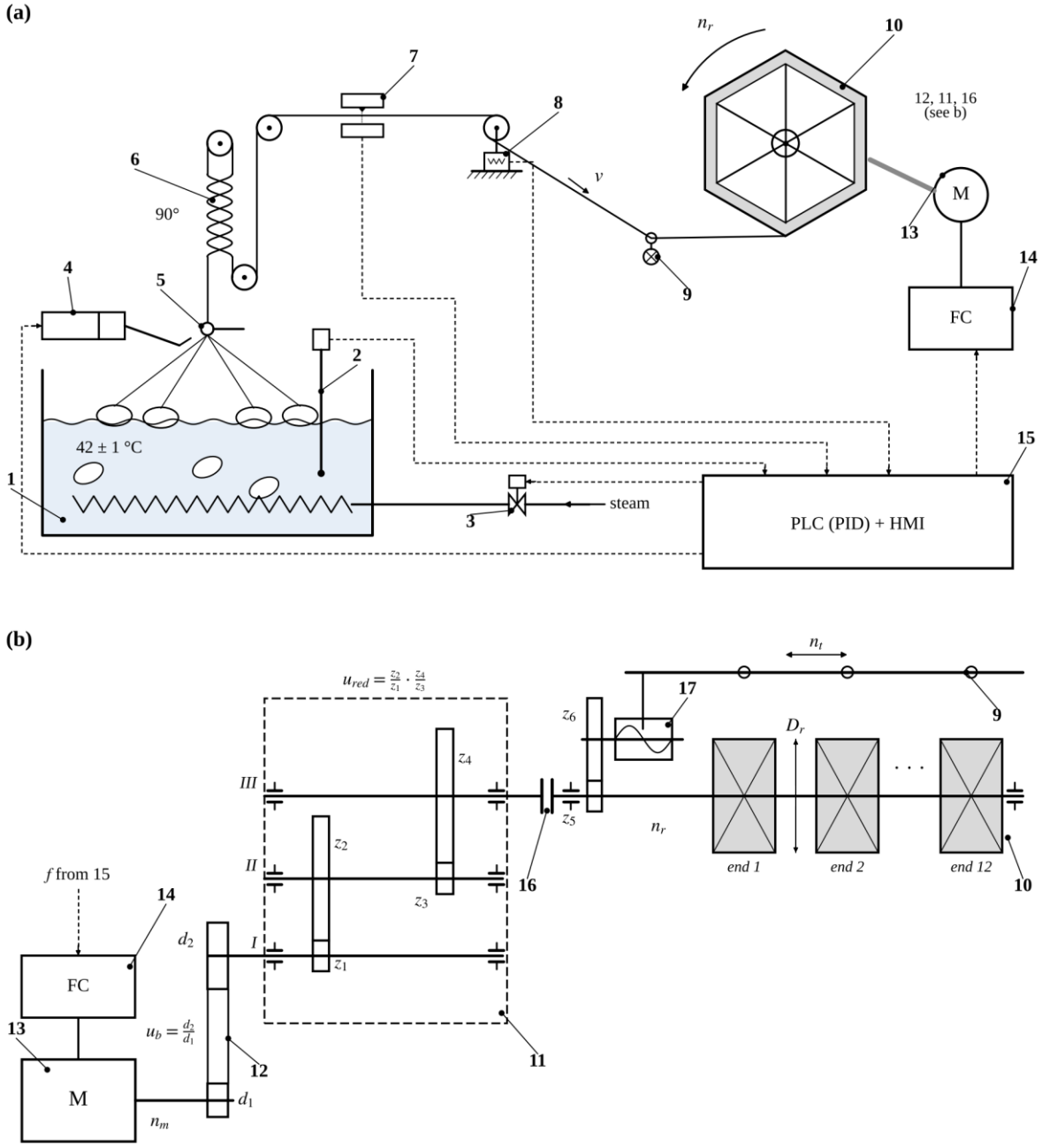


Fig. 2. Scheme of the improved reeling unit: (a) structural scheme of a reeling position; (b) kinematic scheme of the reel drive

1 - reeling basin; 2 - PT100 temperature sensor; 3 - steam heater with proportional valve; 4 - pneumatic cocoon feeder; 5 - ceramic eyelet; 6 - cross-twist (chambon) unit; 7 - photoelectric fineness sensor; 8 - guide roller on load cell; 9 - traverse guide; 10 - take-up reel; 11 - two-stage cylindrical gear reducer; 12 - V-belt drive; 13 - asynchronous motor; 14 - frequency converter (FC); 15 - PLC with HMI; 16 - coupling; 17 - cylindrical cam of the traverse; I, II, III - reducer shafts; dashed lines - signal connections

The reels of the twelve ends of a section are fixed on a common shaft, which is driven by the asynchronous motor 13 through the V-belt drive 12, the two-stage cylindrical gear reducer 11 and the coupling 16 (Fig. 2b). The motor is supplied by the frequency converter 14, whose output frequency is the manipulated variable of the tension loop: the controller output computed by Eq. (1) from the load-cell signal changes the supply frequency and, through the reducer, the angular speed of the reels. The traverse guides of all ends are mounted on a common rod, which is reciprocated by the cylindrical cam

17 driven from the reel shaft through the gear pair z_5/z_6. The total transmission ratio of the drive from the motor to the reel shaft is the product of the ratios of the belt drive and of the two reducer stages,

$$u_\Sigma = u_\mathrm{b} \cdot u_\mathrm{red} = \frac{d_2}{d_1} \cdot \frac{z_2}{z_1} \cdot \frac{z_4}{z_3} \tag{4}$$

where u_b and u_red are the transmission ratios of the belt drive and of the reducer, d_1 and d_2 are the diameters of the driving and driven pulleys, mm, and z_1, z_2 and z_3, z_4 are the numbers of teeth of the gears of the first and second reducer stages. The rotational speed of the reel when the motor is supplied with frequency f, Hz, is

$$n_\mathrm{r} = \frac{n_\mathrm{m}}{u_\Sigma} = \frac{60 f (1-s)}{p u_\Sigma} \tag{5}$$

where n_m is the rotational speed of the motor, min^{-1}, p is the number of pole pairs and s is the slip. The linear take-up (reeling) speed is therefore

$$v = \pi D_\mathrm{r} n_\mathrm{r} = \frac{60 \pi D_\mathrm{r} f (1-s)}{p u_\Sigma} \tag{6}$$

where D_r is the reel diameter, m. Equation (6) is the kinematic link between the control signal and the process: for a given drive, the reeling speed is directly proportional to the converter frequency.

For the pilot machine, $d_1 = 71$ mm and $d_2 = 142$ mm ($u_\mathrm{b} = 2.0$), $z_1 = 20$, $z_2 = 82$, $z_3 = 19$ and $z_4 = 85$ ($u_\mathrm{red} = 4.10 \cdot 4.47 = 18.34$), so that $u_\Sigma = 36.7$. With a four-pole motor ($p = 2$) running at a slip of about 0.03 under the light reeling load ($n_\mathrm{m} \approx 1455$ min^{-1} at 50 Hz) and a reel diameter $D_\mathrm{r} = 0.48$ m (reel perimeter 1.51 m), Eqs. (5) and (6) give $n_\mathrm{r} = 39.7$ min^{-1} and $v = 59.8$ m/min at 50 Hz. The reference speed of 60 m/min is therefore obtained at $f \approx 50.2$ Hz; a change of the frequency by 1 Hz changes the reeling speed by about 1.2 m/min (2 %), and the working range of the converter, from 30 to 70 Hz, corresponds to reeling speeds of approximately 36 to 84 m/min, which covers all speeds used in Section 3.6. The torque on the reel shaft and the power required from the motor are

$$T_\mathrm{r} = T_\mathrm{m} u_\Sigma \eta_\Sigma, \qquad \eta_\Sigma = \eta_\mathrm{b} \eta_\mathrm{g}^2 \eta_\mathrm{br}^3 \tag{7}$$

$$P_\mathrm{m} = \frac{N_\mathrm{e} F v + T_\mathrm{f} \omega_\mathrm{r}}{\eta_\Sigma}, \qquad \omega_\mathrm{r} = \frac{\pi n_\mathrm{r}}{30} \tag{8}$$

where T_m is the motor torque, N·m; $\eta_\mathrm{b} = 0.96$, $\eta_\mathrm{g} = 0.98$ and $\eta_\mathrm{br} = 0.99$ are the efficiencies of the belt drive, of one gear stage and of one pair of rolling bearings, so that $\eta_\Sigma \approx 0.89$; $N_\mathrm{e} = 12$ is the number of ends driven by the shaft; F is the filament tension per end, N; T_f is the friction torque of the reel shaft line, N·m; and ω_r is the angular velocity of the reel, s^{-1}. At $F = 1.0$ cN the useful winding power $N_\mathrm{e} F v$ is only about 0.12 W, and with an estimated friction torque $T_\mathrm{f} \approx 2.5$ N·m the steady-state power demand calculated by Eq. (8) is about 12 W. The 0.25 kW motor was therefore selected by the start-up of the reel group: according to Eq. (7), its rated torque of about 1.7 N·m corresponds to about 57 N·m on the reel shaft, i.e. more than twenty times the steady-state load torque. Owing to this reserve, the reel speed is practically independent of the load and is set solely by the converter frequency through Eq. (6), which is the prerequisite for the accurate tension control reported in Section 3.2. The traverse rod performs

$$n_\mathrm{t} = n_\mathrm{r} \frac{z_5}{z_6} \tag{9}$$

double strokes per minute. With $z_5 = 17$ and $z_6 = 61$, $n_\mathrm{t} \approx 11.1$ min^{-1} and the reel makes 3.59 revolutions per double stroke of the traverse. Because this ratio is not an integer, successive layers of thread are displaced along the skein, which prevents ribbon winding and the sticking of adjacent layers that would otherwise increase the number of breaks during re-reeling.

Experimental design and procedure

Each of the five cocoon lots was divided into two equal halves, one reeled on the baseline machine and the other on the improved machine. Each combination of lot and machine was repeated three times, giving 30 reeling runs in total. The target product was 20/22 den raw silk, which corresponds to approximately seven to eight cocoons per end, and reeling speed was 60 m/min for both machines. Each

run lasted 60 min with 12 ends in operation, and the operators were rotated randomly between machines to reduce the influence of individual skill. Water quality (hardness and pH) was held constant in all runs, since mineral content is known to modify sericin swelling during cooking.

2.6 Measured indicators and test methods

Reelability was defined as the ratio of the number of cocoons from which the filament could be unwound to the end, expressed as a percentage of the number of cocoons fed. Raw silk recovery was determined as the mass of dry raw silk divided by the mass of dry cocoons processed. The number of breaks per 100 m of filament was recorded by the PLC and verified by observation. Fineness was measured on 100 m skeins and the coefficient of variation (CV) was calculated from 40 short-length measurements per run, using a capacitance-based evenness tester. Tenacity and elongation at break were determined on a constant-rate-of-extension tensile tester with a gauge length of 250 mm and a crosshead speed of 250 mm/min, on 30 specimens per run, after conditioning for 24 h at 20 °C and 65 % RH, which is the standard textile atmosphere. Cleanness and neatness were evaluated visually on the black board by a panel of three trained graders and expressed in points, and the overall grade was assigned according to the commercial scheme used by the local reeling association. Thermal energy consumption was calculated from the measured steam flow and was expressed in MJ per kilogram of raw silk.

Statistical analysis

The data were analyzed by two-way analysis of variance with machine type and cocoon lot as factors, followed by paired t-tests of the machine effect within lots. Normality was checked by the Shapiro-Wilk test and homogeneity of variance by Levene's test. The significance level was $\alpha = 0.05$, and results are reported as mean values. Effect sizes were computed as the percentage change relative to the baseline.

To ensure that the differences between the machines were not caused by measurement artefacts, all sensors were calibrated before each experimental day. The PT100 probes were checked against a reference thermometer in a stirred water bath at 40, 60 and 90 °C, and the load cell was calibrated with certified masses in the range of 0 to 50 cN. The optical fineness sensor was calibrated using reference filaments of known linear density, produced by reeling a defined number of cocoons and determining the mass of a 100 m length on an analytical balance. The repeatability of the tensile tester was assessed by testing a reference polyester yarn ten times, which gave a coefficient of variation below 2 %. Skeins were randomly coded, and the graders were not informed about the machine on which each skein had been produced, so that grading was carried out blind. These measures follow the recommendations on reeling control and testing summarized in [17] and [9], and they were adopted in order to ensure that the improvements reported below are attributable to the equipment and not to the experimental procedure.

Results

The five cocoon lots had a mean cocoon mass of 1.92-2.17 g, a mean shell mass of 0.43-0.50 g and a shell ratio of 21.8-23.6 %. The proportion of defective cocoons ranged from 6.1 % to 9.4 %. The differences among lots were statistically significant for the cocoon mass ($p < 0.05$) but did not interact significantly with the machine factor, which indicates that the differences between the two machines were consistent across lots. The shell ratio and filament characteristics are in the range reported for Bombyx mori cocoons in the literature, which confirms that the local material is suitable for reeling into high-grade raw silk[10].

On the improved machine, the PID loop kept the basin temperature within ±1.0 °C of the setpoint during 97 % of the logged time, compared with 52 % on the baseline machine. The tension peaks during cocoon replenishment were reduced from 2.1-2.6 times to 1.2-1.4 times the average tension, and the mean delay between a fineness drop and cocoon addition decreased from 6.4 s to 1.3 s. As a result, the number of filament breaks fell from 3.8 to 1.6 per 100 m, a reduction of 58 %. The classification of break causes showed that the share of breaks caused by thermal non-uniformity decreased from 31 % to 9 %, that caused by tension peaks from 24 % to 8 %, and that caused by guide damage from 18 % to 5 %, while the share of breaks inherent to cocoon defects, which cannot be removed by equipment, rose in relative terms to more than 60 %[11-12].

The principal quality indicators for both machines are given in Table 2 and Fig. 3. All the differences were statistically significant at $p < 0.05$, and for the majority of indicators at $p < 0.01$. Reelability increased by 15.2 percentage points and raw silk recovery by 4.7 percentage points, which is a direct economic benefit because fewer cocoons are wasted as waste silk. The coefficient of variation of fineness decreased from 14.2 % to 7.8 %, and Fig. 3b shows that the fineness trace of the improved machine remained within the ±1 den target band for the great majority of the observation period, whereas the baseline trace repeatedly left the band[13-14].

Table 2. Comparison of baseline and improved machines (mean of 15 runs per machine)

Indicator	Baseline	Improved	Change	p-value
Reelability, %	71.2	86.4	+21.3 %	< 0.001
Raw silk recovery, %	34.9	39.6	+13.5 %	0.004
Breaks per 100 m	3.8	1.6	−57.9 %	< 0.001
Fineness CV, %	14.2	7.8	−45.1 %	< 0.001
Tenacity, cN/dtex	3.42	3.91	+14.3 %	0.008
Elongation at break, %	17.8	20.6	+15.7 %	0.012
Cleanness, points	91.5	95.8	+4.7 %	0.006
Neatness, points	90.2	94.9	+5.2 %	0.009
Thermal energy, MJ/kg silk	410	291	−29.0 %	0.002
Commercial grade	2A-3A	4A-5A	—	—

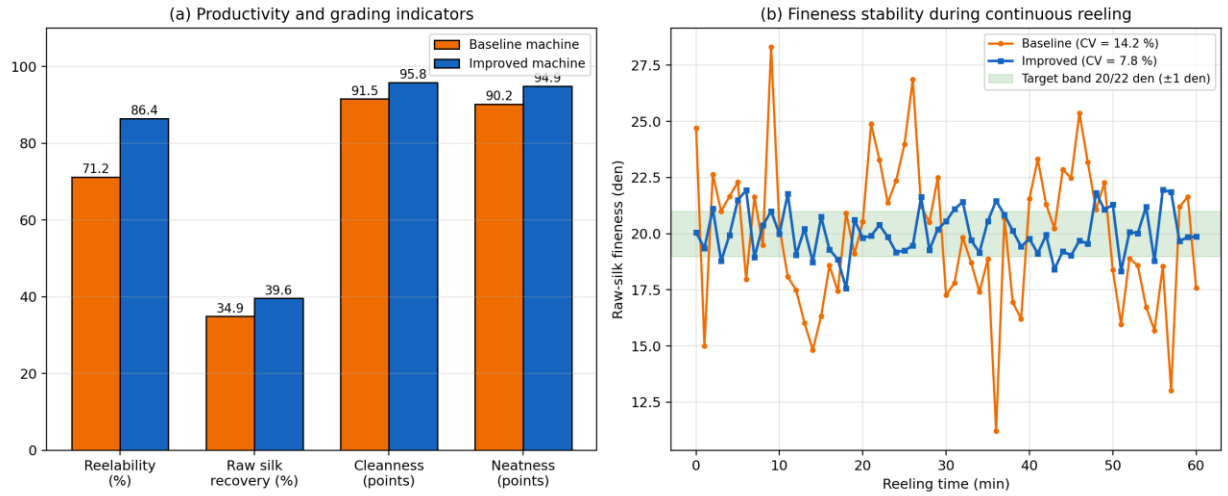


Fig. 3. (a) Productivity and grading indicators and (b) fineness stability during continuous reeling for the baseline and improved machines

Mechanical properties were also improved. Tenacity increased from 3.42 to 3.91 cN/dtex and elongation from 17.8 % to 20.6 %. Because the improved machine used the same cocoons, this gain cannot be associated with a change in the raw material; it is rather the consequence of a more uniform thermal history, lower and steadier tension and a lower density of surface damage on the filament. The Weibull analysis of the tensile data showed that the shape parameter m increased from 7.9 for the baseline silk to 11.6 for the improved silk, which means that the scatter of strength narrowed substantially and the weakest-link failures in subsequent weaving or knitting should become less frequent[15].

Energy consumption and economic implications

The specific thermal energy consumption decreased from 410 to 291 MJ per kilogram of raw silk. The savings came from three sources: the precise control of water temperature eliminated overheating of the basin, the staged cooking system re-used the hot water from the third zone in the first zone, and the drying chamber with humidity control shortened the drying time by approximately 18 %. When these savings are combined with the higher recovery and the higher commercial grade, a first estimate suggests that the additional income per tonne of cocoons processed exceeds the capital cost of the sensors, controller and ceramic components within a single reeling season for a medium-sized enterprise.

The economic estimate was based on a simple model in which the annual benefit equals the sum of the revenue gain from the higher recovery, the price premium of the higher commercial grade and the energy saving, minus the annualized cost of the retrofit. For a line processing 40 tonnes of fresh cocoons per season, the higher recovery alone corresponds to approximately 1.9 tonnes of additional dry raw silk per hundred tonnes of dry cocoons, and the grade improvement allows the product to be sold at the price level of the upper grade category. The sensitivity of the payback period to the price premium was moderate, and even when the premium was halved the investment remained recoverable within two seasons. These figures should be considered indicative, and they should be refined with enterprise-specific cost data, but they show that the technical improvements are also economically rational[16].

Contribution of the individual modules

In order to estimate the contribution of each module, an additional series of reeling runs was performed in which the improved machine was operated with one module at a time returned to its baseline condition (a leave-one-out design, with three runs per condition on the first cocoon lot). The results, summarized in Table 3, show that the largest single effect on the variation coefficient of fineness resulted from disabling the optical fineness control (M5) and the basin temperature control (M3), while the largest increase in breaks followed the replacement of ceramic eyelets by metal guides (M4) and the return to constant-speed take-up (M6). Disabling the humidity-controlled drying (M7) had little effect on the process indicators but resulted in a visible reduction in the elongation at break and in a harsher hand of the skeins. No single module reproduced the full effect of the package, and the sum of the single-module effects was smaller than the total improvement, which indicates synergy among the modules; for example, stable temperature (M3) and stable tension (M6) jointly reduced the incidence of filament sticking, which in turn reduced the load on the fineness controller (M5)[17].

Table 3. Leave-one-out analysis of module contributions (first cocoon lot, mean of three runs)

Module returned to baseline	Fineness CV, %	Breaks per 100 m	Reelability, %
None (full improved machine)	7.6	1.5	87.0
M1 Sorting	8.9	1.7	83.4
M2 Staged cooking	8.3	2.0	80.9
M3 Temperature control	10.8	2.3	82.1
M4 Ceramic eyelets / cross-twist	9.1	2.9	84.2
M5 Fineness sensor and feeder	12.0	1.9	85.0
M6 Adaptive take-up	9.4	2.8	84.7
M7 Humidity-controlled drying	7.9	1.5	86.8
Baseline machine (all modules off)	14.0	3.7	70.6

Sensitivity of quality to operating parameters

The sensitivity of the main quality indicators to the operating parameters was explored by varying one parameter at a time around the optimum on the improved machine. When the basin temperature was raised from 42 °C to 50 °C, the number of breaks increased by 34 % because of excessive swelling of sericin, which produced soft, fragile filaments and promoted sticking between adjacent layers; when it was lowered to 35 °C, the cohesion between the two fibroin brins decreased, the filament was more difficult to unwind, and the fineness variation rose by 22 %. A similar optimum was observed for the reeling speed: increasing the speed from 60 to 80 m/min raised the production rate by one third but also raised the break rate by 41 %, even with adaptive take-up, and therefore 60 m/min was kept as the reference speed. The tension setpoint showed a shallow optimum around 0.9 to 1.1 cN per filament end: below this range the filament lacked sufficient orientation and the skein was loose and uneven, above it the probability of breakage predicted by Eq. (3) increased rapidly. These results show that the equipment improvements allow the process to operate in a well-defined window, and that a closed-loop system is necessary to keep the process inside this window.

Discussion

The results confirm that a substantial fraction of the quality loss observed when reeling local cocoons on conventional equipment is of technical rather than biological origin. The gains in reelability, strength and uniformity were obtained with the same cocoon lots, which isolates the role of the equipment. This agrees with the view that the properties of silk fibres are strongly modulated by processing conditions, as evidenced by the large variation in mechanical properties reported for individual Bombyx mori filaments and by the improved performance of silk drawn under controlled conditions . It also agrees with the structural picture of cocoon silk as a protein composite whose crystalline fraction and orientation develop during spinning and are sensitive to subsequent thermal and mechanical stresses.

Among the seven modules, the temperature control (M3) and the fineness control (M5) contributed most to the reduction of the variation coefficient, while the combination of ceramic eyelets (M4) and adaptive take-up (M6) made the largest contribution to the reduction in breaks and fuzz. The capstan relation (Eq. 2) provides a simple explanation: reducing μ from 0.35 to 0.18 lowers the tension gain over a given wrap angle by more than a third, so that the filament experiences a lower mean and peak tension along the whole path. The Weibull model (Eq. 3) shows why these matters, since the breakage probability depends on a high power of the ratio between tension and characteristic strength, and a modest reduction of peak tension results in a disproportionately large decrease in the break rate.

The staged cooking in M2 deserves particular attention. Sericin is a heterogeneous group of proteins with different solubilities, and the outer sericin layers are more soluble than those close to the fibroin core. A single-stage high-temperature cooking dissolves the outer layers rapidly and can leave the inner layers hard, producing uneven unwinding, whereas a graded profile allows water to penetrate the shell before the temperature reaches its maximum. The higher reelability and the lower share of breaks caused by hard-glued layers observed in our experiments support this mechanism, which is also consistent with the architecture of the cocoon shell as a layered non-woven structure with varying sericin content described in.

From the practical standpoint, the improvement package is attractive for small and medium enterprises because it does not require replacement of the whole machine. Sensors, ceramic parts and a compact PLC can be retrofitted to existing frames, and the control algorithm is simple enough to be tuned by plant engineers. Moreover, the higher grade achieved by raw silk from local cocoons increases the competitiveness of domestic producers relative to imported raw silk and opens opportunities in markets where high-grade silk is demanded for textiles and for emerging applications, including medical and technical products. As the quality of regenerated fibroin materials depends on the quality of the starting fibre and on the degumming process, uniform and well-reeled raw silk is also an advantage for these downstream uses[18].

The quantitative improvement in strength deserves a short comment in the context of the intrinsic properties of the fibre. The tenacity values achieved here remain well below those of the best forced-silking filaments, and a gap between the performance of the natural fibre and that of the reeled raw silk is inevitable because the raw silk consists of several filaments that do not carry the load uniformly, and because sericin, which is a non-load-bearing component, contributes to the cross-section. However, the narrower strength distribution found on the improved machine, expressed by the higher Weibull modulus, is relevant for downstream processing, since weaving and knitting are limited by the weakest sections of the yarn rather than by its mean strength. The reduction of mechanical damage to the surface of the filament probably contributed to this effect, in the same way that surface defects are known to control the strength variability of other brittle and semi-crystalline fibres.

A further point concerns the transferability of the findings to other cocoon sources. The variability in mechanical and physical properties among silkworm breeds, rearing seasons and even individual cocoons is large, and the optimum set of operating parameters is therefore not universal. For this reason, the control architecture proposed here, in which temperature, fineness and tension setpoints are held in the PLC and can be changed through the human-machine interface, is more important than the specific numerical values reported in Table 1. We recommend that each enterprise carries out a short calibration campaign, comparable with the sensitivity analysis described in Section 3.6, whenever a new cocoon hybrid or a new batch of cocoons with markedly different shell ratio is introduced. The data collected by the logger during such campaigns would also be a natural basis for statistical process control, in which the control limits for fineness and tension are updated continuously.

Finally, it is useful to place the energy results in perspective. Silk reeling is a thermally intensive operation, because cooking, basin heating and drying all involve hot water or hot air, and a considerable share of the cost of raw silk is related to energy. The 29 % reduction obtained here originates mainly from the elimination of overheating and from heat recovery rather than from a fundamental change of the process, so that further improvements are probable through the use of heat pumps, insulated basins and solar pre-heating of process water. Because these measures can be combined with the instrumentation presented in this work, the improved reeling line can be regarded as a platform for the gradual modernization of the silk industry based on local raw material[19].

A final consideration relates to the operation and maintenance of the improved line. Ceramic eyelets are hard but brittle, and chipped edges can damage the filament as severely as worn metal; they should therefore be inspected at least once per shift by passing a cotton thread through the eyelet. Load cells and optical sensors drift slowly and should be recalibrated at the intervals used in this study. Operators need only short training to use the human-machine interface, since the main routine tasks, loading cocoons and clearing local faults, are not changed. In the pilot enterprise, the training required was two working days per operator, and the operators reported that the continuous display of temperature and tension helped them to detect developing faults earlier than before.

The environmental dimension of the upgrade should also be mentioned. Lower specific energy consumption directly reduces the combustion of fuel for steam generation, and the higher reelability reduces the amount of waste silk and of cocoon residue that must be treated or discarded. In addition, the staged cooking system re-uses process water, so that the volume of effluent containing dissolved sericin is reduced. Sericin, which is released into cooking and degumming liquors, is a valuable protein with documented applications in biomaterials and cosmetics, and its more concentrated and cleaner recovery from the reeling effluent could create an additional revenue stream for the enterprise. In this respect, the improved reeling line contributes not only to quality and productivity but also to a more circular use of the silkworm cocoon, in which all its protein fractions are valorized.

Several limitations should be acknowledged. First, the study was limited to five cocoon lots from a single rearing season, so the interaction with seasonal variation, rearing conditions and hybrid type needs to be explored in further work. Second, the visual grading of cleanness and neatness retains a subjective element, although the use of a trained panel limited its effect. Third, the economic assessment is preliminary and does not include maintenance and calibration costs, which may be significant in

environments with unstable power supply or hard water. Future research should address machine-learning based adaptive tuning of the PID gains, in-line optical inspection of defects, the extension of the approach to automatic reeling machines, and a full life-cycle assessment of the energy and water savings that the improved system provides.

Conclusion

This study demonstrated that an integrated set of seven equipment improvements, comprising cocoon sorting, staged cooking, closed-loop basin temperature control, ceramic eyelets with an optimized cross-twist unit, an optical fineness sensor with automatic cocoon feeding, an adaptive load-cell take-up and humidity-controlled drying, significantly improves the quality of raw silk obtained from local silkworm cocoons. On the improved machine, reelability rose from 71.2 % to 86.4 %, recovery from 34.9 % to 39.6 %, the variation of fineness fell from 14.2 % to 7.8 %, breaks per 100 m were reduced by 58 %, tenacity rose by 14.3 % and the product reached the top commercial grade, while the specific thermal energy consumption decreased by 29 %.

The findings show that the quality limit of local cocoons is often set by the equipment rather than by the biological material, and that modest, instrumented retrofits can remove this limit. The design rules established here, namely a basin temperature tolerance of ±1 °C, a tension peak ratio below 1.4, a fineness correction delay below 1.5 s and a low-friction guide path, can be adopted by other reeling enterprises. The kinematic calculation of the reel drive ($u_{\Sigma} = 36.7$) showed that the reeling speed is proportional to the converter frequency, about 1.2 m/min per hertz, which provides the tension loop with a simple and precise actuator. Further work on more cocoon lots, on hybrid-specific tuning of process parameters and on automatic control based on adaptive algorithms is recommended.

References

[1] C. Holland, K. Numata, J. Rnjak-Kovacina, and F. P. Seib, “The biomedical use of silk: Past, present, future,” Adv. Healthcare Mater., vol. 8, no. 1, Art. no. 1800465, 2019.\

[2] D. N. Rockwood, R. C. Preda, T. Yücel, X. Wang, M. L. Lovett, and D. L. Kaplan, “Materials fabrication from Bombyx mori silk fibroin,” Nature Protocols, vol. 6, no. 10, pp. 1612–1631, 2011.\

[3] F. Vollrath and D. P. Knight, “Liquid crystalline spinning of spider silk,” Nature, vol. 410, no. 6828, pp. 541–548, 2001.\

[4] Z. Shao and F. Vollrath, “Surprising strength of silkworm silk,” Nature, vol. 418, no. 6899, p. 741, 2002.\

[5] H.-J. Jin and D. L. Kaplan, “Mechanism of silk processing in insects and spiders,” Nature, vol. 424, no. 6952, pp. 1057–1061, 2003.\

[6] Y.-Q. Zhang, “Applications of natural silk protein sericin in biomaterials,” Biotechnol. Adv., vol. 20, no. 2, pp. 91–100, 2002.\

[7] J. G. Hardy, L. M. Römer, and T. R. Scheibel, “Polymeric materials based on silk proteins,” Polymer, vol. 49, no. 20, pp. 4309–4327, 2008.\

[8] M. Mondal, K. Trivedy, and S. Nirmal Kumar, “The silk proteins, sericin and fibroin in silkworm, Bombyx mori Linn.—a review,” Caspian J. Environ. Sci., vol. 5, no. 2, pp. 63–76, 2007.\

[9] K. M. Babu, Silk: Processing, Properties and Applications. Cambridge, U.K.: Woodhead Publishing, 2013.\

[10] G. H. Altman, F. Diaz, C. Jakuba, T. Calabro, R. L. Horan, J. Chen, H. Lu, J. Richmond, and D. L. Kaplan, “Silk-based biomaterials,” Biomaterials, vol. 24, no. 3, pp. 401–416, 2003.\

[11] C. Vepari and D. L. Kaplan, “Silk as a biomaterial,” Prog. Polym. Sci., vol. 32, no. 8–9, pp. 991–1007, 2007.\

[12] T. D. Sutherland, J. H. Young, S. Weisman, C. Y. Hayashi, and D. J. Merritt, “Insect silk: One name, many materials,” Annu. Rev. Entomol., vol. 55, pp. 171–188, 2010.\

[13] F. G. Omenetto and D. L. Kaplan, “New opportunities for an ancient material,” Science, vol. 329, no. 5991, pp. 528–531, 2010.\

[14] H.-P. Zhao, X.-Q. Feng, and H.-J. Shi, “Variability in mechanical properties of Bombyx mori silk,” Mater. Sci. Eng. C, vol. 27, no. 4, pp. 675–683, 2007.\

[15] F. Chen, D. Porter, and F. Vollrath, “Structure and physical properties of silkworm cocoons,” J. R. Soc. Interface, vol. 9, no. 75, pp. 2299–2308, 2012.\

[16] C.-Z. Zhou, F. Confalonieri, N. Medina, Y. Zivanovic, C. Esnault, T. Yang, M. Jacquet, J. Janin, M. Duguet, R. Perasso, and Z.-G. Li, “Fine organization of Bombyx mori fibroin heavy chain gene,” Nucleic Acids Res., vol. 28, no. 12, pp. 2413–2419, 2000.\

[17] Y. F. Lee, Silk Reeling and Testing Manual, FAO Agricultural Services Bulletin 136. Rome, Italy: Food and Agriculture Organization of the United Nations, 1999.\

[18] B. Kundu, R. Rajkhowa, S. C. Kundu, and X. Wang, “Silk fibroin biomaterials for tissue regenerations,” Adv. Drug Deliv. Rev., vol. 65, no. 4, pp. 457–470, 2013.\

[19] F. Rustamova, S. Dadajonov, and U. B. Akhunbabayev, “From local silkworm seeds achievement processed fine-fiber cocoons processing of low-linear density raw silk release technology,” Oscar Journal of Applied Science and Technology, vol. 5, no. 12, pp. 147–151, 2025.